Experimental evaluation of a digitized fiber-wireless system employing sigma delta modulation

Luis M. Pessoa,[1,*] **Joana S. Tavares,**[1] **Diogo Coelho**[1,2] **and Henrique M. Salgado**[1,2]

[1]*INESC TEC - INESC Technology and Science (formerly INESC Porto), Porto, Portugal*
[2]*Faculty of Engineering, University of Porto, Portugal*
[*]*luis.m.pessoa@inesctec.pt*

Abstract: Digitized radio-over-fiber (D-RoF) transport schemes are being pointed as viable alternative solutions to their analog counterparts, in order to avoid distortion/dynamic range problems. Here we propose a novel D-RoF architecture that takes advantage of a bandpass sigma-delta modulator at the transmitter which subsequently permits the usage of a simpler/cheaper base station that avoids the employment of a digital to analog converter. The proposed architecture exploits the properties of the digital signal to enable the extraction of an higher carrier frequency through the employment of a bandpass filter. Furthermore, we present a comprehensive analysis regarding the impact of a low-cost electro-optic modulation on the quality of received demodulated signal. Finally, a comparison performance analysis between the conventional D-RoF and the proposed architecture is presented. We conclude that although the proposed architecture performs similarly to conventional D-RoF schemes, it is more competitive for either upgrading installed systems as well as for new deployments.

OCIS codes: (060.4510) Optical communications; (060.5625) Radio frequency photonics; (060.2360) Fiber optics links and subsystems.

References and links

1. J. O'Reilly, P. Lane, J. Attard, and R. Griffin, "Broadband wireless systems and networks: an enabling role for radio–over–fibre," Phil. Trans. R. Soc. A. **358**, 2297–2308 (2000).
2. C. Lim, A. Nirmalathas, M. Bakaul, P. Gamage, K.-L. Lee, Y. Yang, D. Novak, and R. Waterhouse, "Fiber-wireless networks and subsystem technologies," J. Lightw. Technol. **28**, 390–405 (2010).
3. Z. Jia, J. Yu, G. Ellinas, G.-K. Chang, "Key Enabling Technologies for Optical?Wireless Networks: Optical Millimeter-Wave Generation, Wavelength Reuse, and Architecture," J. Lightw. Technol., **25**, 3452–3471 (2007).
4. J. Yu, G.-K. Chang, Z. Jia, A. Chowdhury, M.-F. Huang, H.-C. Chien, Y.-T. Hsueh, W. Jian, C. Liu, Z. Dong, "Cost-Effective Optical Millimeter Technologies and Field Demonstrations for Very High Throughput Wireless-Over-Fiber Access Systems," J. Lightw. Technol. **28**, 2376–2397 (2010).
5. K.-i. Kitayama, T. Kuri, J. V. Olmos, and H. Toda, "Fiber-wireless networks and radio-over-fibre technique," IET Conference on Lasers and Electro-Optics and Conference on Quantum Electronics and Laser Science. CLEO/QELS 2008, pp. 1–2 (2008).
6. T. Kurniawan, A. Nirmalathas, C. Lim, D. Novak, and R. Waterhouse, "Performance analysis of optimized millimeter-wave fiber radio links," IEEE Trans. Microwave Theory Tech. **54**, 921–928 (2006).
7. P. M. Wala, "A new microcell architecture using digital optical transport," IEEE Vehicular Technology Conference, pp. 585–588 (1993).
8. G. E. Betts, "Linearized modulator for suboctave-bandpass optical analog links," IEEE Trans. Microwave Theory Tech. **42**, 2642–2649 (1994).

#211180 - $15.00 USD Received 1 May 2014; revised 5 Jun 2014; accepted 8 Jun 2014; published 11 Jul 2014

9. S. K. Korotky, and R. M. de Ridder, "Dual parallel modulation schemes for low-distortion analog optical transmission," IEEE J. Select. Areas Commun. **8**, 1377–1381 (1990).
10. R. B. Childs, and V. A. O'Byrne, "Predistortion linearization of directly modulated DFB lasers and external modulators for AM video transmission," Optical Fiber Communication Conference, p. WH6. (1990).
11. (X. Zhang, B. Lee, C.-y. Lin, A. X. Wang, A. Hosseini, and R. T. Chen, "Highly Linear Broadband Optical Modulator Based on Electro-Optic Polymer," IEEE Photon. J. **4**, 2214–2228 (2012).
12. P. Li, L. Yan, T. Zhou, W. Li, Z. Chen, W. Pan, and B. Luo, "Improved linearity in down-converted analog photonic link by polarization manipulation," Opt. Lett. **39**, 2641–2644 (2014).
13. A. Nirmalathas, P. A. Gamage, C. Lim, D. Novak, and R. Waterhouse, "Digitized radio-over-fiber technologies for converged optical wireless access network," J. Lightw. Technol. **28**, 2366–2375 (2010).
14. A. Nirmalathas, P. Gamage, C. Lim, D. Novak, R. Waterhouse, and Y. Yang, "Digitized rf transmission over fiber," IEEE Microwave **10**, 75–81 (2009).
15. P. A. Gamage, A. Nirmalathas, C. Lim, D. Novak, and R. Waterhouse, "Design and analysis of digitized rf-over-fiber links," J. Lightw. Technol. **27**, 2052–2061 (2009).
16. P. A. Gamage, A. Nirmalathas, C. Lim, D. Novak, and R. Waterhouse, "Experimental demonstration of the transport of digitized multiple wireless systems over fiber," IEEE Photon. Technol. Lett. **21**, 691–693 (2009).
17. P. Gamage, A. Nirmalathas, C. Lim, D. Novak, and R. Waterhouse, "Simultaneous transmission of digitized multiple wireless services over optical fiber," National Fiber Optic Engineers Conference, Optical Society of America, (2009).
18. Y. Yang, C. Lim, and A. Nirmalathas, "Multichannel digitized rf-over-fiber transmission based on bandpass sampling and FPGA," Trans. Microwave Theory Tech. **58**, 3181–3188 (2010).
19. P. Kiss, J. Arias, D. Li, and V. Boccuzzi, "Stable high-order delta-sigma digital-to-analog converters," IEEE Trans. Circuits Syst. I, Reg. Papers1 **51**, 200–205 (2004).
20. T. Salo, "Bandpass delta-sigma modulators for radio receivers," Ph.D. thesis, Helsinki University of Technology (2003).
21. S. Hein and A. Zakhor, "On the stability of sigma delta modulators," IEEE Trans. Signal Processing **41**, 2322–2348 (1993).
22. K. Lear, V. Hietala, H. Hou, M. Ochiai, J. Banas, B. Hammons, J. Zolper, and S. Kilcoyne, "Small and large signal modulation of 850 nm oxide-confined vertical cavity surface emitting lasers," Osa Trends Opt Photo **15**, 69–74 (1997).

1. Introduction

The ever increasing demand for bandwidth in wireless mobile communications is a challenging problem. Researchers are currently addressing solutions that involve, for example, maximizing the spectral efficiency, taking advantage of alternative bands of the spectrum as well as considering smaller cells, which involves employing a high number of base-stations (BSs) to achieve spatial re-utilization of the spectrum. Radio-over-Fiber (RoF) [1] techniques are considered today as very promising to facilitate the backhauling of a large number of remote antennas, enabling the shifting of the hardware complexity from the BS to the control station (CS). RoF consists in transporting the radio signals over optical fiber by means of an optical carrier between a remote site/BS and the head-end/CS node of the cellular network [2–5], in a completely transparent, frequency/protocol agnostic manner. RoF links where an optical carrier is modulated by (multiple) analog radio signals, known as analog RoF (A-RoF) inherently suffer from inter-modulation distortion (IMD) arising from the nonlinearities incurred in both radio-frequency (RF) and optical components [6]. Figure 1 depicts a typical A-RoF scheme. It has been shown that IMD is the main performance limiting factor in A-RoF transmissions, affecting the link dynamic range which also decreases linearly with the optical fiber length due to attenuation [7, 8]. Furthermore, this problem becomes more challenging when A-RoF is combined with the widely used orthogonal division multiplexing (OFDM) modulation, due to its inherently high vulnerability to nonlinear distortion. However, several analog methods have been proposed to suppress the IMD in analog transmitting systems and devices, including the usage of two integrated-optical modulators operated in parallel [9], by applying a predistorted signal to the nonlinear components [10] as well as by polarization manipulation using two phase modulators [12]. Digitized radio-over-fiber (D-RoF) transport schemes that merge both optical and electronic digitization worlds are being studied and pointed as viable alternative solutions

#211180 - $15.00 USD Received 1 May 2014; revised 5 Jun 2014; accepted 8 Jun 2014; published 11 Jul 2014

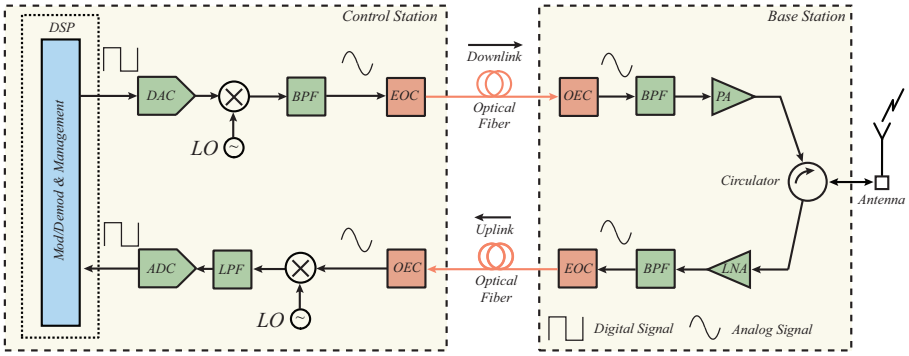

Fig. 1. Diagram of a generic radio-over-fiber architecture.

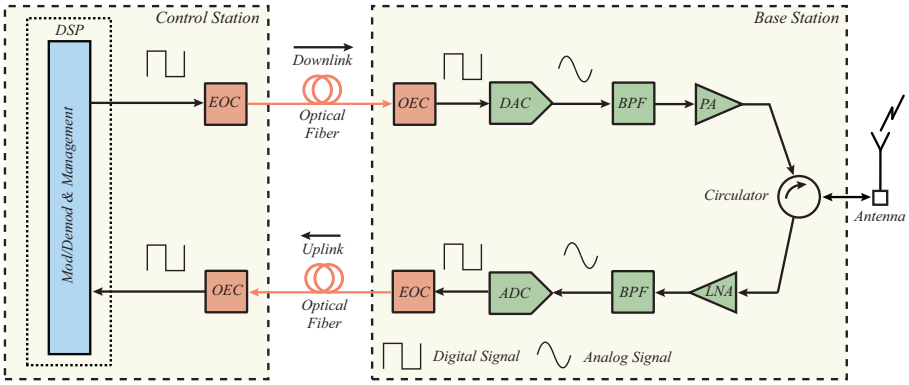

Fig. 2. Diagram of a standard digitized radio-over-fiber architecture.

to A-RoF systems [13]. D-RoF has been first proposed in 1993 [7] but only during the last ten years it has receiving growing attention thanks to the increasing speed of electronics [14]. In Fig. 2 a typical digitized RoF scheme is depicted.

D-RoF requires the usage of high bandwidth Analog-to-Digital (ADC) converters at the transmit side and Digital-to-Analog (DAC) converters at the receive side. Contrary to analog systems, by employing D-RoF the IMD is avoided and the dynamic range of the system remains constant and irrespective of the optical fiber length, provided that the received signal amplitude is above the sensitivity of the link [15–17]. Bandpass sampling is used in D-RoF schemes to lower the sampling rate requirements since most common wireless standards (e.g., WiMAX, WiFi, 3G, 4G) have small fractional bandwidths relative to their carrier frequencies [14, 18]. Optical links employing digitized transport of RF signals with both CS and BSs having digital interfaces open the possibility of designing backhaul networks seamlessly integrated with both existing and future broadband optical networks [17, 18].

Although D-RoF schemes are an interesting alternative to their analog counterparts, the fact that the remote site requires the employment of a high bandwidth DAC is a considerable disadvantage, and therefore the existence of a viable alternative would be desirable. Here we propose a novel solution for the implementation of future RoF systems based on the usage of a bandpass sigma-delta (SD) modulator at the transmitter side, working as a 1-bit ADC. The proposed

#211180 - $15.00 USD Received 1 May 2014; revised 5 Jun 2014; accepted 8 Jun 2014; published 11 Jul 2014

digital transmission solution combines advantages of both digital and analog schemes. In the downlink the RF signal is digitized and transported over the optical fiber as a stream of bits, which, as mentioned, provides advantages in terms of IMD and dynamic range. However, contrarily to traditional D-RoF schemes, at the BS the DAC is avoided, decreasing the BS's cost and complexity and power consumption. By using a SD modulator as ADC, the DAC at the BS can be suppressed since its equivalent operation is performed by means of a simple bandpass filter (BPF).

In this paper we show, according to the best of our knowledge, the world's first digitized RoF solution avoiding the employment of a DAC at the receiver, and capable of achieving RF carrier signals in the GHz region by extracting high frequency signal replicas that arise due to properties of the SD based digital transmission over fiber. Furthermore, we present a comprehensive analysis regarding the impact of a low-cost vertical cavity surface emitting laser (VCSEL) based electro-optic modulation on the quality of received demodulated signals, in particular we address key design trade-offs regarding the impact of the laser bias current operating point as well as the optical modulation extinction ratio and overshoot of the modulated pulse. Additionally, we investigate the impact of taking advantage of high frequency replica signals that arise (due to the properties of the SD modulator) to overcome the need of high bitrate SD modulators. Note that a VCSEL was considered since it is a low-cost EOC widely available that is increasingly being used and also due to the fact that the top-ranked publications in the D-RoF topic also use VCSEL, thus facilitating a comparative analysis [13–17]. Additionally, state-of-the-art VCSELs are currently supporting digital signal transmissions up to 10 Gbps, which is more than 5 times the 1.8 Gbps bitrate presented in this work. Therefore, these cost effective and still high-performance VCSEL based links are a good compromise solution for the proposed architecture.

The paper is organized as follows: in section 2 we review the fundamentals of sigma-delta modulation; in section 3 the proposed SD based RoF concept, the experimental setup used for performance evaluation and the experimental results are presented and discussed; in section 4 we present a comparative analysis between the proposed architecture and the conventional D-RoF; and finally section 5 draws the conclusions.

2. Sigma-Delta Modulator (SDM) review

The sigma-delta modulator lays in the group of modulators that use oversampling and a feedback loop to reduce the noise in the band of interest [19]. Additionally, the quantization noise spectrum is shaped and high signal-to-noise ratio (SNR) values in the band of interest may be achieved. The SD modulator consists of a loop-filter composed by an integrator, a quantizer and a digital-to-analog converter (DAC) in the feedback path. By increasing the oversampling rate of the modulator, we are in fact spreading the noise over the frequency spectrum. Additionally, the feedback loop acts as a filter, contributing to the noise shaping effect. By increasing the number of feedback loops (or equivalently, the order of the modulator), it is possible to optimize the noise shaping in order to decrease the noise level in the band of interest. We start by analyzing low-pass prototype structures, both first and higher order, from which a bandpass structure can be derived.

2.1. First-order structure

Figure 3 represents a generic block diagram of the first order sigma-delta modulator. The modulator consists of a loop-filter composed by an integrator, a quantizer and a digital-to-analog converter (DAC) in the feedback path.

From the literature [19], the signal and noise transfer functions (STF and NTF) are given by, respectively:

#211180 - $15.00 USD Received 1 May 2014; revised 5 Jun 2014; accepted 8 Jun 2014; published 11 Jul 2014

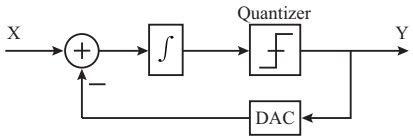

Fig. 3. Sigma-Delta modulator block diagram, having a 1st order structure.

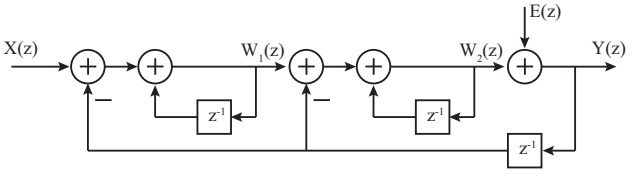

Fig. 4. Equivalent 2nd order Sigma-Delta modulator linear model.

$$STF(z) = 1 \tag{1}$$

$$NTF(z) = 1 - z^{-1} \tag{2}$$

While $STF(z)$ is equal to the unity, the magnitude of $NTF(z)$ is actually shaped by a high-pass filter.

2.2. High-order structure model

By increasing the number of feedback loops, it is possible to further optimize the noise shaping in order to achieve an higher SNR in the band of interest. A second order SD modulator can be obtained by simply cascading two first order elements (see Fig. 4). Equivalently, it can also be obtained by substituting the quantizer in Fig. 3 by another first order modulator.

In Fig. 5(a) the squared magnitude of the noise shaping function for modulators with orders $L = 1, 2$ and 3 is shown. It can be observed that the noise shaping function acts as a high-pass filter, where the higher the order, the lower the quantization noise at lower frequencies.

Figure 5(b) shows the normalized noise power as a function of the maximum frequency of a low-pass signal for modulators with orders up to three. As previously referred, the high-pass behavior of the noise shaping function pushes the noise to higher frequencies. Furthermore, for the LP structures, it is considered that $f_{max} \ll f_s$ and $OSR = f_s/(2f_{max})$, where OSR represents the oversampling rate (OSR), f_{max} the maximum frequency of the signal and f_s the sampling frequency. It can be seen that the noise power decreases as the OSR and/or the order of the modulator increases. In particular, by increasing the sampling frequency by a factor of 2, it can be seen that the noise power is reduced by factors 9, 16 and 21 dB for orders one, two and three, respectively.

The previously described SD modulators are low-pass prototype structures. In the next section we show the procedure for obtaining a bandpass structure starting from the analyzed low-pass prototypes.

2.3. Bandpass modulator structure

With minor changes, the SD modulator structure derived in the previous sections can be applied to RF bandpass signals having $f_{max}/fs \gg 1$ [20]. In fact, the high-pass characteristic of the

#211180 - $15.00 USD Received 1 May 2014; revised 5 Jun 2014; accepted 8 Jun 2014; published 11 Jul 2014

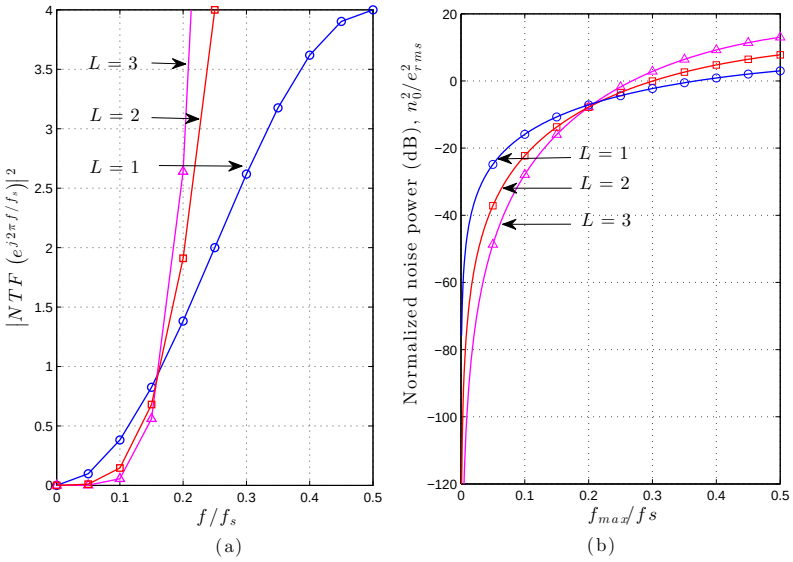

Fig. 5. (a) Squared magnitude of the noise shaping function, (b) Normalized noise power in the band of interest as a function of the maximum frequency (signal bandwidth)

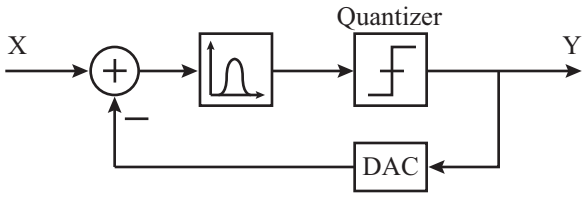

Fig. 6. Equivalent band-pass sigma-delta modulator linear model.

noise shaping function can be transformed into a stop-band function with zeros located at the center frequency of the input signal. Moreover, the OSR only depends on the signal bandwidth, being given by $OSR = f_s/(2BW)$, BW being the two-sided bandwidth of the RF signal, while for the low-pass structure the BW term is replaced by f_{max} as shown before. The NTF filter characteristic can be obtained by designing a bandpass filter with zeros away from DC instead of the integrator used in the LP version (see Fig. 6).

The simplest way to design a BP SD modulator is to start with a LP prototype. By applying a pseudo 2-path transformation to a LP NTF, a BP NTF with zeros at $f_c = f_s/4$ is obtained. This transformation is performed by substituting $z \rightarrow -z^2$. This ensures the stability properties of the LP structure are preserved [19, 21]. By placing the signal carrier frequency at $f_s/4$, the sampling frequency is automatically dictated. Moreover, a LP to BP transformation is always accomplished by an increase of the order of the modulator, i.e., a nth-order LP modulator originates in fact a $2n$th-order BP modulator.

#211180 - $15.00 USD Received 1 May 2014; revised 5 Jun 2014; accepted 8 Jun 2014; published 11 Jul 2014

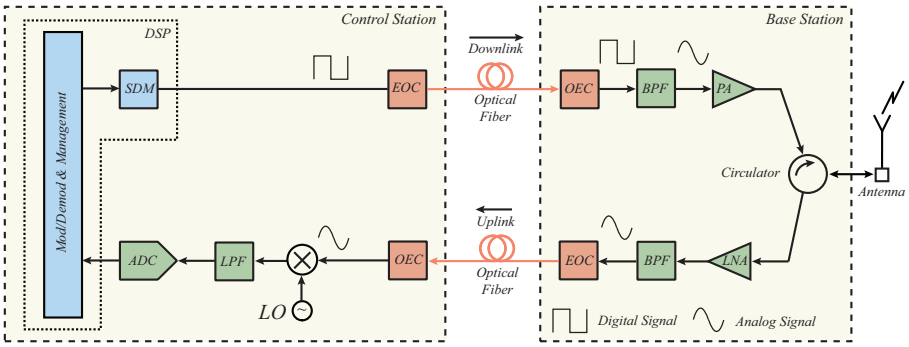

Fig. 7. Diagram of the proposed SD based D-RoF architecture, with the uplink consisting, as an example, of a conventional A-RoF scheme.

3. Proposed SDoF system

The here proposed SD-over-fiber (SDoF) system architecture is more advantageously applicable to the downlink path of a RoF link, since the employment of a DAC is avoided at the BS, which not only represents a cost reduction but it also means that future upgrades in terms of increased carrier frequency or modulation format are automatically accommodated. Furthermore, by avoiding the DAC the power consumption is reduced at the BS. In fact, a conventional D-RoF system employing a DAC at the BS is limited by its front-end analog bandwidth and resolution, which may preclude future upgrades. Figure 7 shows a possible implementation of the proposed scheme, where the uplink consists of a conventional A-RoF scheme, although any desired uplink architecture could be employed. The proposed downlink architecture is comprised of a completely digital transmitter at the CS that takes advantage of the digital signal processing implementation of a SD modulator to convert the digital representation of the analog wireless signal into a NRZ bit stream. At the CS, all of the analog blocks such as up/down frequency converters and mixers can be implemented in the digital domain jointly with the SD modulator blocks (DAC, NTF filter, quantizer) in a single platform. Similarly to D-RoF schemes, this completely digital architecture allows an improved flexibility in the digital implementation of any desired functions at the CS. Still at the CS, an electro-optic converter (EOC) is used to modulate an optical carrier with the digital signal. The EOC may consist of a direct modulation of a laser (used in this work), or of an external optical modulator, depending on the required digital signal bitrate. Then at the BS, a photodiode (PD) acts as an optical to electrical converter (OEC), followed by a bandpass filter (BPF) tuned to the RF signal center frequency, then by an RF power amplifier (PA), and finally by an RF circulator and RF antenna. Figure 8 depicts the normalized power spectrum of the bandpass SD modulated signal obtained at the output of the DSP. Due to the nature of the Non Return to Zero (NRZ) line code given by the zero-order hold (ZOH) and the sampling process, the spectrum of the digital signal repeats every f_s, where f_s stands for the sampling frequency of the 1-bit ADC of the bandpass SD modulator, generating high frequency replicas of the original RF signal. The bitrate of the SD modulator is then given by $R_b = f_s \times bit$, enabling the transmission of sub-Gbps digital streams from which RF signals centered at the Gigahertz frequency region can be obtained with no additional frequency up-conversion hardware at the BS. Figure 8 clearly shows the original RF signal (f_{c0}) at $f_s/4$, as well as two high frequency replicas f_{c1} and f_{c2} at $f_s + f_{c0}$ and $2f_s + f_{c0}$, respectively, as well as their image frequency components. For example, assuming the availability of DSP with 10 Gbps capability as well as cost-effective EOC and OEC components, the maximum RF

#211180 - $15.00 USD Received 1 May 2014; revised 5 Jun 2014; accepted 8 Jun 2014; published 11 Jul 2014

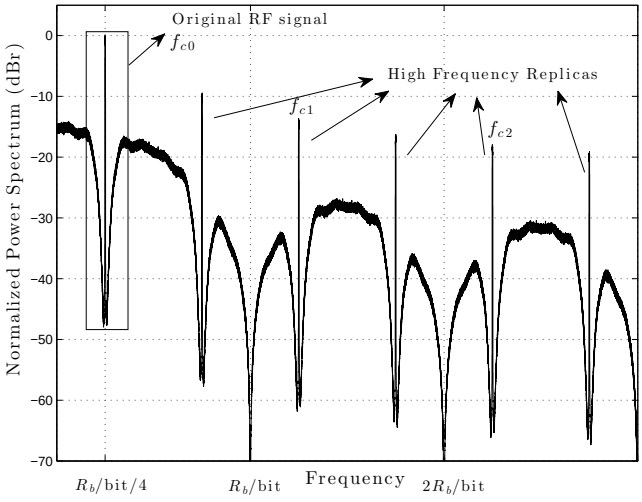

Fig. 8. Normalized power spectrum of the BP SD modulated signal obtained at the output of the DSP.

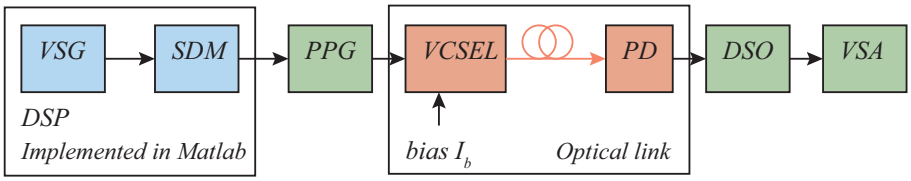

Fig. 9. Experimental Setup used for evaluating the performance of the proposed SDoF architecture.

signal bandwidth would be 100 MHz for an OSR of 50, and the fundamental frequency would be at 2.5 GHz, the first replica at 12.5 GHz and the second replica at 22.5 GHz. Another advantage of this SD based D-RoF downlink architecture is that it allows the transmission of both traditional analog as well as the proposed SD modulated signals over the same network since the hardware at BSs is simultaneously compatible with both approaches. Therefore, currently installed A-RoF deployments could be migrated to the proposed SD based D-RoF architecture without replacing BSs, while only the downlink path of the control station would need to be upgraded. On the contrary, the transition to a traditional D-RoF architecture would require the upgrading all of BSs. Furthermore, as for future deployments targeting all-digital networks, the proposed SD based D-RoF architecture could be readily employed, with the advantage of avoiding the employment of the DAC in BSs.

3.1. SDoF experimental setup

For proof-of-concept purposes, we consider the point-to-point downlink transmission employing the proposed SD modulator based RoF architecture as previously presented in Fig. 7. The experimental setup used to evaluate the proposed system is illustrated in Fig. 9. The RF signal is generated at a digital signal processor (DSP) emulated by a PC running Matlab, corresponding

#211180 - $15.00 USD Received 1 May 2014; revised 5 Jun 2014; accepted 8 Jun 2014; published 11 Jul 2014

to the vector signal generator (VSG) block. The 1-bit ADC operation is performed by means of a $4th$ order $fs/4$ BP SD modulator implementation in Matlab. Then, an Agilent N4906B Serial BERT is used as a pulse pattern generator (PPG) to directly modulate the 1550 nm VCSEL. After passing through the optical fiber, the bit stream is converted into the electrical domain by means of a photodiode performed by an Agilent 81495A reference receiver. Since there is no need of DAC front-end components at the BS, the digital signal is directly sampled by means of an Agilent DSO90254A oscilloscope running a vector signal analysis (VSA) software. Note that we have considered an optical fiber channel with only a few tens of meters since chromatic dispersion and nonlinear effects are out of the scope of this work.

Table 1 summarizes the characteristics of the four SD bit streams used in order to evaluate the system performance. The RF signal digitized by the 1-bit ADC is a 16-QAM modulated sinewave centered at a given frequency. Two main 1-bit SD streams (#1 and #2) and two additional bit streams (#3 and #4) with 1.8 times the SD bitrate of the original ones are considered. Note that signal #3 and #4 have the same OSR than #1 and #2, respectively. However, their bandwidth are 1.8 times higher and their corresponding center frequency is also higher. The 1.8 multiplication factor was chosen in order to have a f_{c1} of signals #3 and #4 equal to f_{c2} of signals #1 and #2.

Table 1. Characteristics of transmitted signals

Signal	#1	#2	#3	#4
SDM Bitrate (Gbps)	1	1	1.8	1.8
OSR	50	100	50	100
RF BW (MHz)	10	5	18	9
RF f_{c0} (MHz)	250	250	450	450
RF f_{c1} (MHz)	1250	1250	2250	2250
RF f_{c2} (MHz)	2250	2250	4050	4050

3.2. SDoF system results

In this section we assess the performance of the proposed SDoF concept using the experimental setup presented in section 3.1.

Let us first consider the transmission of SD signal #1. In order to evaluate the link, we have considered the Modulation Error Ratio (MER) performance metric obtained through the VSA. Figure 10 depicts the MER of the received and bandpass filtered 16-QAM signal centered at the fundamental frequency f_{c0} = 250 MHz, as well as at higher frequencies given by replicas f_{c1} = 1.25 GHz and f_{c2} = 2.25 GHz, as a function of the peak-to-peak (pp) input voltage (V_{pp}) of the transmitted SD bit stream. Furthermore, Fig. 10 also shows the impact of the bias current on the performance. From these results we can conclude that the performance increases with bias current and that there is an optimum value (or range of values) of V_{pp} where the optimum performance is achieved. For low V_{pp} values the amplitude of the signal is low and, thus, the MER is mainly limited by the additional noise sources introduced by the optical channel such as thermal, shot and relative intensity noises (RIN). For high V_{pp} values the amplitude of the SD signal imposes a sub-threshold zero level modulation at the VCSEL, which results in a pattern dependent turn-on jitter (as well as increased turn-on delay) and overshoot [22]. This translates into the distortion of the digital signal waveform. It is also important to highlight that the maximum MER achieved in a back-to-back configuration, i.e., without the optical channel, is approximately 47 dB, which is very close to the MER obtained with a bias current of

#211180 - $15.00 USD Received 1 May 2014; revised 5 Jun 2014; accepted 8 Jun 2014; published 11 Jul 2014

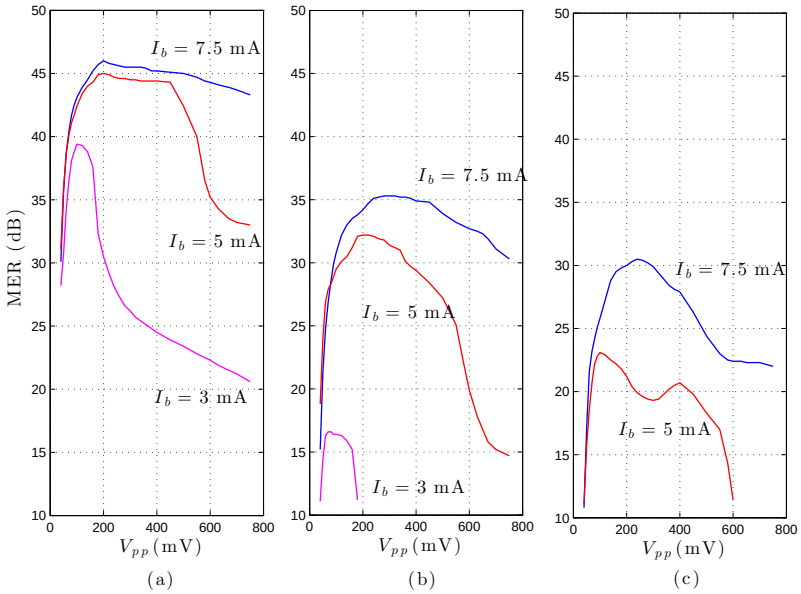

Fig. 10. MER as a function of the input pp amplitude considering different bias currents for the RF signal centered at (a) 250 MHz; (b) 1.25 GHz and (c) 2.25 GHz.

7.5 mA. Another relevant result is the performance decrease with the increase of the chosen replica center frequency. This effect can be explained by the signal insertion loss due to the ZOH frequency response. Since the optical channel introduces additional noise, a decrease of the MER is expected. Figure 11 represents the maximum MER achieved as a function of the bias current, for signals #1 to #4. As expected, the MER of signals #2 and #4 is higher than the that of signals #1 and #3 since the OSR of the former is higher than that of the latter. It is interesting to note that the maximum MER values for both fundamental frequency (f_{c0}) values are very similar. This result indicates that the increase of the SD bitrate has no impact on the performance. However, if we consider f_{c1} of signals #1 and #3 for instance, a significant difference is observed. This result indicates the presence of a frequency dependent optical channel related noise, which is expectedly dominated by the laser RIN. In fact, measurements of the VCSEL RIN level were performed at 1.25 GHz and 2.25 GHz and an increase of 5 dB was verified, from -143 dB/Hz to -138 dB/Hz. In order to understand the impact of the distortion induced by the optical channel (mainly by the VCSEL) on the transmitted digital signal and particularly on the performance of the received RF signal, Fig. 12 shows the amplitude of the received digital signal (after the PD) for three input voltages at a constant bias current of 5 mA. As it can be seen, as the input voltage increases, so does its output amplitude and the previously referred overshoot effect and turn-on delay. Figure 13 depicts both the overshoot and the extinction ratio (ER) of the received digital signal. As shown, the ER, overshoot and turn-on jitter increase drastically at very low input voltages for a low bias current value of 3 mA. For a bias of 5 mA, a more relaxed increase of these values is reported. The impact of these effects on the performance of the RF signal conveyed in the SD bit stream can be understood by analyzing its spectrum. Figure 14 shows received spectra of the RF signal centered at f_{c0} for bias currents of 3 mA and 5 mA and considering the same input voltages as in Fig. 12. From this result it is clear that the pulse distortion has a noise adding effect in the received RF signal, i.e., as the overshoot and turn-on jitter increases, a noise component arises at the RF signal's band. This

#211180 - $15.00 USD Received 1 May 2014; revised 5 Jun 2014; accepted 8 Jun 2014; published 11 Jul 2014

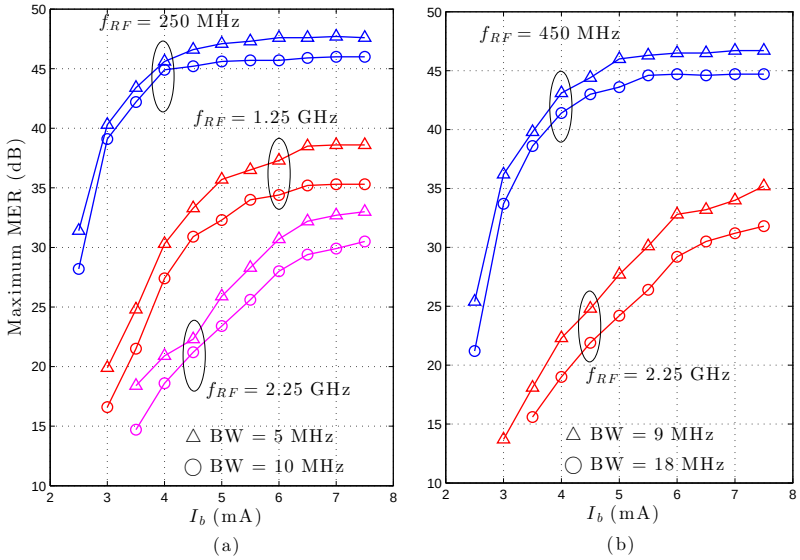

Fig. 11. Maximum MER achievable as a function of bias current at different frequencies and bandwidths. (a) R_b = 1 Gbps; (b) R_b = 1.8 Gbps.

result is in-line with those shown in Figs. 10 and 11 for the MER. Furthermore, Table 2 shows the measured single tone spurious free dynamic range (SFDR) using a SDM bitrate of 1 Gbps, V_{pp} = 280 mV and I_b=7.5 mA, and considering a signal bandwidth of 10 MHz. The results show the degrading effect introduced by the optical link, namely due to the optical link attenuation as well as VCSEL distortion and the photodiode built-in amplifier distortion.

Table 2. Measured SFDR

Frequency	w/o optical link (dBc)	w/ optical link (dBc)
250 MHz	80.3	61.4
1250 MHz	69.0	48.5
2250 MHz	63.3	47.6

Finally, in order to understand the impact of the transmission over optical fiber on the quality of the received signal, a simulation was conducted in Matlab, where the electric field of the SDM signal was affected with the effect of fiber chromatic dispersion (with a dispersion coefficient of 17 ps/nm.km) at a wavelength of 1550 nm. A simulation was performed instead of an experimental assessment due to unavailability of a sufficient length of optical fiber. The simulation included a band-limiting third order Bessel filter with a 3 dB frequency equal to the SDM bitrate, and the square law response of the photodiode. Other laser and photodiode degrading effects were not included, since the purpose was to evaluate only the impact induced by the optical fiber on transmission. The degradation of system performance was assessed by means of the MER parameter. The results shown in Fig. 15 include the replica frequency f_{c1} from the 1 Gbps SDM signal and replica frequencies f_{c1} and f_{c2} from the 1.8 Gbps SDM signal, considering an OSR of 50. From the results it can be concluded that the impact of fiber dispersion

#211180 - $15.00 USD Received 1 May 2014; revised 5 Jun 2014; accepted 8 Jun 2014; published 11 Jul 2014

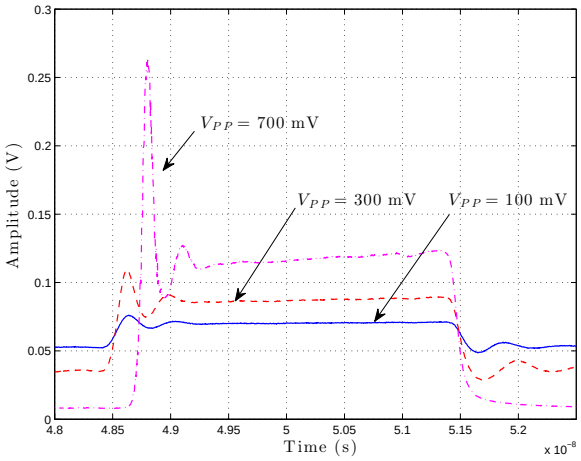

Fig. 12. VCSEL overshoot effect at a I_b = 5 mA, considering an input signal with three amplitudes.

becomes only significant for fiber lengths above 50 km, even for the higher frequency replica considered. This means that for typical RoF applications the impact of fiber transmission is expected to be negligible.

4. D-RoF vs SDoF comparative analysis

It is important to understand how the SDoF architecture compares with the typical D-RoF systems. For that, we have carried out an equivalent experimental evaluation of a conventional D-RoF (see Fig. 2) link using the same VCSEL and photodiode as in the SDoF.

4.1. D-RoF experimental setup

The experimental setup is illustrated in Fig. 16. Here, the signal modulator/demodulator, frequency up/down converter and ADC/DAC operations are performed at a DSP emulated by a PC running Matlab. The pattern generator used is also the same Agilent N4906B Serial BERT, which guarantees similar conditions. The received digital bit sequence is retrieved by the pattern detector module of the Serial BERT that optimally employs the bit decision operation. The RF signal is considered to be a 16-QAM, centered at 2.475 GHz, with a symbol rate of 5 MS/s. The VCSEL was biased at 6.25 mA to ensure the necessary bandwidth and the extinction ratio was set to 10 dB.

4.2. Results and discussion

Figure 17 depicts the spectra of the output of the DAC considering a sampling frequency, f_s, of 125 MHz and different quantization bits, N_b. As it can be seen, the noise power decreases log-linearly at a rate of (theoretically) 6.02 dB with N_b down to the level where the jitter noise starts to dominate. It can also be seen the attenuation caused by the frequency roll-off of the DAC. In Fig. 18 a performance evaluation using the MER metric is depicted as a function of the ADC sampling frequency for ADC/DAC with 7 quantization bits and for two clock jitter noise levels. As expected, the performance decreases with the jitter noise. Additionally, in can

#211180 - $15.00 USD Received 1 May 2014; revised 5 Jun 2014; accepted 8 Jun 2014; published 11 Jul 2014

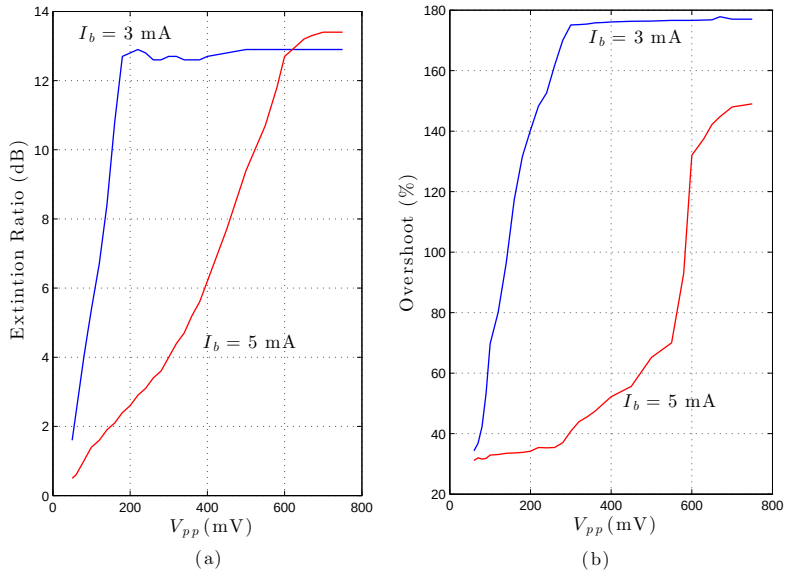

Fig. 13. (a) Extintion ratio, (b) overshoot and (c) jitter of the received signal considering two bias currents as a function of the input *pp* amplitude.

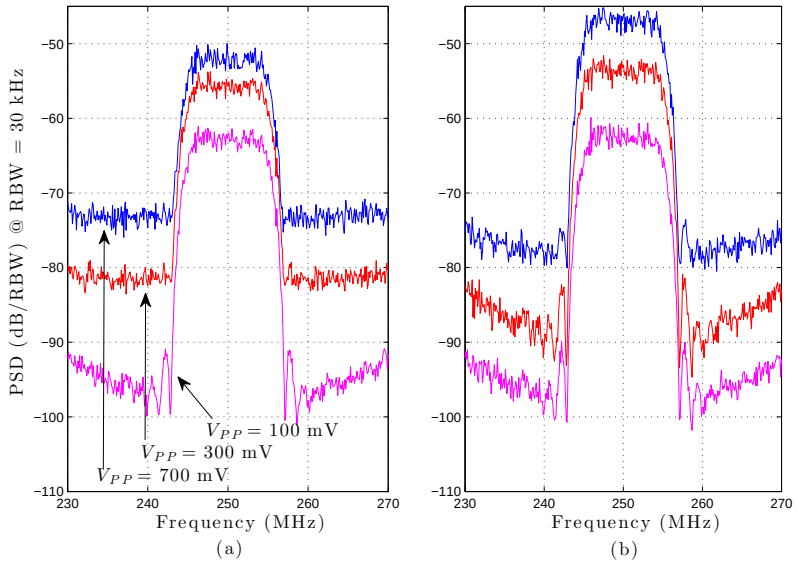

Fig. 14. Power spectrum densities of the received signal centered at 250 MHz considering three input *pp* amplitude values for (a) I_b = 3 mA and (b) I_b = 5 mA.

#211180 - $15.00 USD Received 1 May 2014; revised 5 Jun 2014; accepted 8 Jun 2014; published 11 Jul 2014

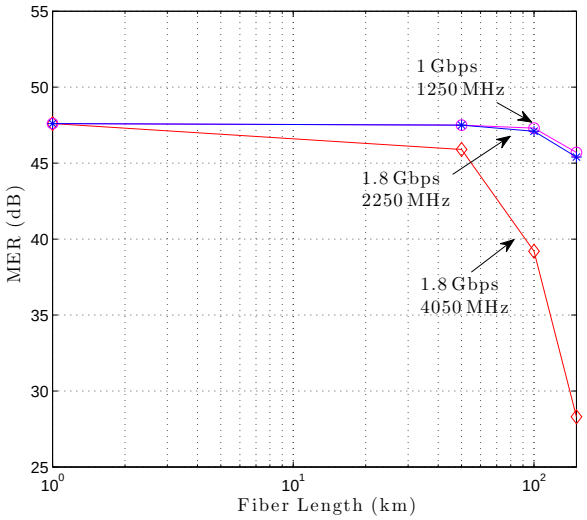

Fig. 15. MER achieved as a function of optical fiber length due to fiber chromatic dispersion.

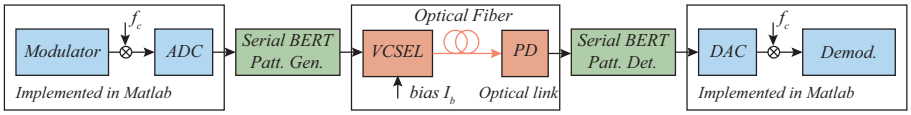

Fig. 16. Experimental Setup used for evaluating the performance of the conventional D-RoF architecture.

be seen that the MER of the signal is severely affected for low ADC sampling frequencies due to the frequency roll-off effect of the DAC.

As it can be seen, results indicate MER values of 28 dB considering f_s of 125 MHz and 7 quantisation bits (with no jitter) producing a digital link with a total bitrate of 875 Mbps. For a MER of 35.5 dB the sampling frequency would need to be increased to 375 MHz, resulting in a total bitrate of 2.625 Gbps. On the other hand, SDoF results reported above, specifically in Fig. 11, indicate maximum MER levels of 32 dB at 2.25 GHz using a digital link with a bitrate of 1 Gbps. Moreover, literature results for similar D-RoF systems (e.g. [14, 15]) indicate MER values no higher than 32 dB, which are also in agreement with the ones presented here.

From these results we can argue that the performance of the proposed SDoF architecture is at least equivalent to that of the conventional DRoF concept, while featuring the above-mentioned advantages, namely avoiding the employment of the DAC at the BS and making maintenance and upgrade tasks more easier and less expensive.

5. Conclusion

A novel sigma-delta modulator based digitized radio-over-fiber architecture was proposed and experimentally evaluated. Analog modulated signals having bandwidths between 5 MHz and 18 MHz were digitally transmitted using bitrates of 1 Gbps and 1.8 Gbps and recovered at carrier frequencies up to 2.25 GHz without the need of frequency upconvertion. The results show

#211180 - $15.00 USD Received 1 May 2014; revised 5 Jun 2014; accepted 8 Jun 2014; published 11 Jul 2014

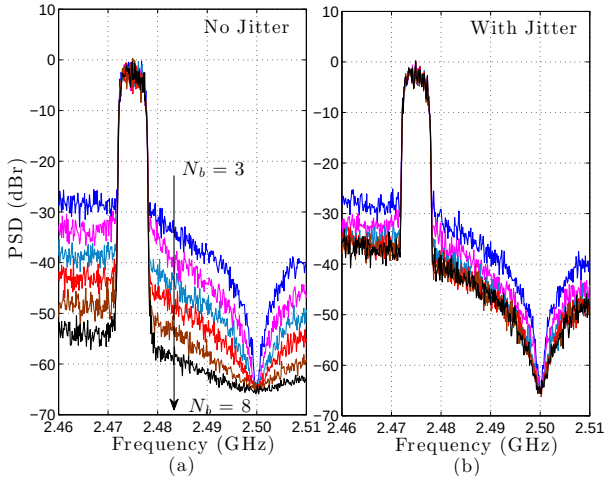

Fig. 17. Measured spectra of the DAC output for different quantisation bits and (a) no jitter and (b) an ADC clock jitter value of 0.8 ps.

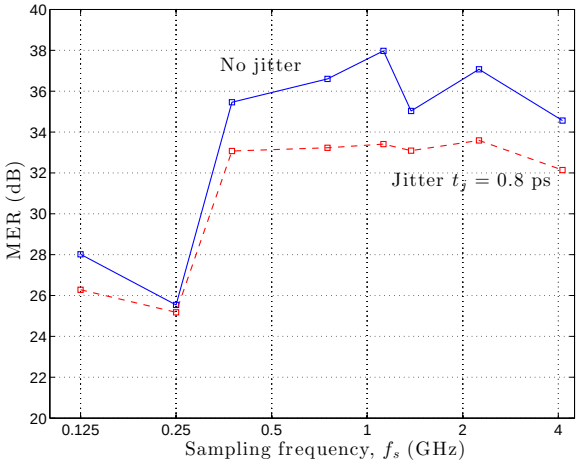

Fig. 18. MER vs ADC/DAC sampling frequency, f_s.

#211180 - $15.00 USD Received 1 May 2014; revised 5 Jun 2014; accepted 8 Jun 2014; published 11 Jul 2014

that better signal-to-noise ratios (above 30 dB @ 2.25 GHz) can be achieved for higher VCSEL bias currents, while the pulse overshoot distortion dictates the employment of an optimum level of VCSEL modulation amplitude for achieving maximum MER. Furthermore, a comparison analysis with a conventional D-RoF system was also presented. We conclude that, while performing similarly to conventional D-RoF schemes, the proposed architecture is economically competitive for either upgrading installed systems as well as for new deployments. Finally, the method has been preliminarily found to be suitable for transmitting OFDM signals, which is currently under investigation and will be the target of a subsequent publication.

Acknowledgment

This work is partly funded by FP7 project Daphne, grant ACP8-GA-2009-233709, by the ERDF through COMPETE Programme and by the FCT within project FCOMP-01-0124-FEDER-022701 and Programme POCTI/FEDER with grant REEQ/1272/EEI/2005 and project FCOMP-01-0124-FEDER-037281. Project "NORTE-07-0124-FEDER-000058" is financed by the North Portugal Regional Operational Programme (ON.2 O Novo Norte), under the National Strategic Reference Framework (NSRF), through the European Regional Development Fund (ERDF), and by national funds, through the Portuguese funding agency, Fundação para a Ciência e a Tecnologia (FCT). The authors also like to thank RayCan for providing the VCSEL for this work.

#211180 - $15.00 USD Received 1 May 2014; revised 5 Jun 2014; accepted 8 Jun 2014; published 11 Jul 2014